MOLECULAR AND CELLULAR BIOLOGY, Sept. 2003, p. 6419–6434 Vol. 23, No. 18
0270-7306/03/$08.00+0 DOI: 10.1128/MCB.23.18.6419–6434.2003

Mice Deficient for Testis-Brain RNA-Binding Protein Exhibit a Coordinate Loss of TRAX, Reduced Fertility, Altered Gene Expression in the Brain, and Behavioral Changes

Vargheese Chennathukuzhi,[1] Joel M. Stein,[2] Ted Abel,[2] Stacy Donlon,[1] Shicheng Yang,[1] Juli P. Miller,[3] David M. Allman,[3] Rebecca A. Simmons,[4] and Norman B. Hecht[1]*

Center for Research on Reproduction and Women's Health,[1] Department of Pathology and Laboratory Medicine,[3] and Department of Pediatrics, Children's Hospital of Philadelphia,[4] School of Medicine, and Department of Biology,[2] University of Pennsylvania, Philadelphia, Pennsylvania

Received 1 April 2003/Returned for modification 6 May 2003/Accepted 28 May 2003

Testis-brain RNA-binding protein (TB-RBP), the mouse orthologue of the human protein Translin, is a widely expressed and highly conserved protein with proposed functions in chromosomal translocations, mitotic cell division, and mRNA transport and storage. To better define the biological roles of TB-RBP, we generated mice lacking TB-RBP. Matings between heterozygotes gave rise to viable, apparently normal homozygous mutant mice at a normal Mendelian ratio. The TB-RBP-related and -interacting protein Translin-associated factor X was reduced to 50% normal levels in heterozygotes and was absent in TB-RBP-null animals. The null mice were 10 to 30% smaller than their wild-type or heterozygote littermates at birth and remained so to about 6 to 9 months of age, showed normal B- and T-cell development, and accumulated visceral fat. TB-RBP-null male mice were fertile and sired offspring but had abnormal seminiferous tubules and reduced sperm counts. Null female mice were subfertile and had reduced litter sizes. Microarray analysis of total brain RNA from null and wild-type mice revealed an altered gene expression profile with the up-regulation of 14 genes and the down-regulation of 217 genes out of 12,473 probe sets. Numerous neurotransmitter receptors and ion channels, including γ-aminobutyric acid A receptor α1 and glutamate receptor α3, were strongly down-regulated. Behavioral abnormalities were also seen. Compared to littermates, the TB-RBP-null mice appeared docile and exhibited reduced Rota-Rod performance.

The mouse nucleic acid-binding protein testis-brain RNA-binding protein (TB-RBP) is the orthologue of the human protein Translin (5, 6, 26). The official nomenclature for the mouse TB-RBP gene is *Tsn*. Translin/TB-RBP is expressed in many organisms, including fission yeasts, plants, frogs, insects, and mammals. In mammalian tissues, it is ubiquitously expressed, with especially high levels in the brain and testis (18, 31, 32). Translin is a 228-amino-acid protein encoded by a single-copy gene on human chromosome 2 (3). TB-RBP, encoded by a single-copy gene on mouse chromosome 1, differs from the human protein in three amino acids (3, 55, 56). Translin has been implicated in DNA rearrangements through binding to single-stranded DNA sequences found at the breakpoint junctions of chromosomal translocations in lymphoid malignancies and solid tumors (26). Electron microscopic and analytical ultracentrifugation studies have revealed multimeric ring structures of Translin which have been proposed to recognize staggered breaks occurring at recombination hot spots in the genome (26, 35, 45, 52). Similar multimeric ring structures are seen when TB-RBP is crystallized (44). Recently, Translin was shown to accelerate cell proliferation when overexpressed in cultured HEK cells (22).

In addition to its proposed roles in DNA recombination and cell proliferation, TB-RBP functions in mRNA transport and/or stabilization and in translational regulation (40, 41). In the brain and testis, TB-RBP serves as a linker protein binding specific mRNAs to microtubules (19, 59). Complexes of TB-RBP in association with specific mRNAs have been found in the nuclei, cytoplasm, and intercellular bridges connecting male germ cells, suggesting roles in both intracellular and intercellular mRNA transport (41). In dendrites, the inhibition of TB-RBP causes the disruption of mRNA sorting for TB-RBP-associated mRNAs (46).

Yeast two-hybrid and immunoprecipitation assays have identified a number of proteins that interact with TB-RBP, including a transitional endoplasmic reticulum ATPase, cytoskeletal γ-actin, and Translin-associated factor X (TRAX) (57). TRAX is a 33-kDa protein with extensive amino acid homology to Translin/TB-RBP (4). In the brain, both TB-RBP and TRAX are expressed in neurons, especially in cerebellar Purkinje cells and in the hippocampus (28, 58). TRAX forms a complex with TB-RBP in neuronal dendrites that has been proposed to be involved in dendritic RNA processing (17). TRAX has also been shown to interact with nuclear matrix protein C1D, which is an activator of DNA-dependent protein kinase (14, 15). This association has supported roles for TRAX in the repair of double-stranded DNA breaks and in V(D)J recombination.

To elucidate the functions of TB-RBP in mammals, we generated mice homozygous for an inactivating mutation of the TB-RBP gene. We found that mice lacking TB-RBP are viable but are growth retarded at birth and show abnormalities in

* Corresponding author. Mailing address: Center for Research on Reproduction and Women's Health, School of Medicine, University of Pennsylvania, 1310 Biomedical Research Building II/III, 421 Curie Blvd., Philadelphia, PA 19104-6142. Phone: (215) 898-0144. Fax: (215) 573-5408. E-mail: nhecht@mail.med.upenn.edu.

fertility and behavior. Gene expression is also markedly altered in the brain. In addition, the absence of TB-RBP in cells leads to a concomitant loss of TRAX at the posttranscriptional level.

MATERIALS AND METHODS

Targeting construct and generation of mice. TB-RBP-null mice were generated from embryonic stem (ES) cells corresponding to OST 63223 (Omnibank Sequence Tag; Lexicon Genetics, Houston, Tex.) targeted by gene trapping. The gene trap vector contained a 5′ retroviral long terminal repeat (LTR), a splice acceptor, βgeo (fusion of β-galactosidase and neomycin phosphotransferase genes), a Bruton tyrosine kinase gene, and a 3′ LTR. Retroviral infection, selection, and screening of ES cells were carried out as described previously (61, 62). ES cells corresponding to OST 63223, containing the first three exons of the TB-RBP gene upstream of βgeo, as detected by 5′ rapid amplification of cDNA ends analysis, were selected for blastocyst injection into C57BL/6 mice to produce chimeric mice. Chimeric males with high proportions of agouti coat color were bred to C57BL/6 females for germ line transmission of the targeted allele. Heterozygous F_1 males were outbred to C57BL/6 females to obtain heterozygous F_2 animals. Heterozygous F_2 animals were bred to homozygosity. Siblings were never used as mating pairs, and homozygous animals were analyzed along with littermate control animals.

DNA preparation and analysis. Genomic DNA samples were prepared from mouse tail clippings by the method of Laird et al. (33). Briefly, tail clippings were digested overnight on a rotating tube rack at 55°C with 0.5 ml of lysis buffer, containing 100 mM Tris-Cl (pH 8.5), 5 mM EDTA, 0.2% sodium dodecyl sulfate (SDS), 200 mM NaCl, and 100 μg of proteinase K/ml. Supernatants from the lysates were centrifuged at 13,000 rpm in an Eppendorf centrifuge for 10 min and then transferred to prelabeled tubes containing 0.5 ml of isopropanol. The DNA was recovered from each of the samples by lifting the precipitates with disposable pipette tips and dissolving the genomic DNA overnight at 55°C in Tris-EDTA buffer (100 μl).

Southern blot analyses were carried out to determine the site of integration of the gene trap sequence in the TB-RBP gene locus and to genotype the mice. A 450-bp probe for genomic Southern blots, selected from the third intron, was generated by PCR amplification from mouse genomic DNA. Genomic DNA samples (10 μg) were digested with *Hin*dIII and electrophoresed in 0.7% agarose gels. Southern blot hybridizations were carried out by standard protocols (42).

A PCR screening strategy with the three primers indicated in Fig. 1A was designed for the DNA samples. The primer sequences were as follows: F1, GGC ATG GCA CAA ATA CTC AAG G; F2, GCA TCT CAC GAC GTC TGG GGA GC, and R1, GTA GCC TTG TTG GAG TAC GTG. A 300-bp amplicon from the wild-type genomic locus and an 1,800-bp amplicon from the targeted allele were amplified with Ready To Go PCR beads (Amersham Pharmacia, Piscataway, N.J.). PCR conditions were as follows: initial denaturation for 5 min at 94°C followed by 35 cycles at 94°C for 30s, 60°C for 30s, and 72°C for 90s.

Serum hormones. The levels of serum follicle-stimulating hormone (FSH) and luteinizing hormone (LH) were measured by radioimmunoassays. Assays were performed at the National Hormone and Peptide Program (Harbor-UCLA Medical Center) by A. F. Parlow, and the results were analyzed by determining means and standard errors of the means (SEMs).

Northern and Western blotting. Total RNAs were prepared from tissue samples from wild-type, heterozygous, and TB-RBP-null littermates with TRIreagent (Sigma, St. Louis, Mo.). RNA samples (10 μg) were separated in 1.5% agarose gels under denaturing conditions. Northern blotting was carried out with cDNA probes as described previously (12, 13). The membranes were reprobed with a β-actin cDNA probe as a loading control.

Tissue samples were homogenized for protein extracts in hypotonic buffer (20 mM HEPES [pH 7.4], 40 mM KCl, 2 mM $MgCl_2$, 2 mM dithiothreitol [DTT], 0.1% NP-40) containing a proteinase inhibitor cocktail (50 μl/100 mg of tissue; Sigma). After centrifugation for 10 min (10,000 × *g*, 4°C), the postnuclear supernatants were used for Western blotting as described previously (12). Briefly, each of the protein samples (30 μg) was electrophoretically separated in 4 to 12% Tris-glycine-SDS-polyacrylamide gradient gels and transferred to Immobilon-P membranes (Millipore, Bedford, Mass.). Affinity-purified anti-TB-RBP and anti-TRAX antibodies were used for Western blot analyses. Peroxidase-conjugated protein A and an enhanced chemiluminescence detection kit (Amersham Pharmacia) were used to detect TB-RBP and TRAX.

Histologic evaluation and TUNEL assay. Testes were prepared for light microscopy by standard methods at the Histology Core Facility of Children's Hospital of Pennsylvania. Immunohistochemical evaluation was performed as previously described (41). Staining by terminal deoxynucleotidyltransferase-mediated dUTP-biotin nick end labeling (TUNEL) of paraffin sections of testes was carried out with an ApopTag peroxidase staining kit (Intergen, Purchase, N.Y.).

Preparation and analysis of cauda epididymidis sperm. Cauda epididymidis sperm were collected from TB-RBP knockout mice and their wild-type littermates as described by Travis et al. (50). Briefly, the caudal sperm were collected in a buffer containing 20 mM Tris-HCl, 130 mM NaCl, and 1 mM EDTA (pH 7.5) at 37°C. The sperm were washed, centrifuged, and resuspended in the same buffer. Total sperm counts were determined with a hemacytometer after appropriate dilutions with deionized water.

Body composition. Body composition was determined by use of dual-laser X-ray absorptiometry (DEXA) (Lunar Corporation, Madison,Wis.). The DEXA scanner was specialized for small animals. The instrument settings used were as follows: a scan speed of 40 mm/s, a resolution of 1.0 by 1.0 mm, and automatic or manual histogram width estimation. The coefficient of variation, as assessed by five repeated measurements (with repositioning of the mouse between the measurements), was less than 5%. Littermates (four of each genotype) from three different litters were analyzed.

RNA isolation and oligonucleotide array expression analysis. Total RNAs from whole brain samples from wild-type and TB-RBP knockout littermates were prepared with TRIreagent. Pooled RNAs from four wild-type and four TB-RBP-null mice were used for cRNA preparation. Microarray analyses were carried out at the Penn Microarray Core Facility (http://www.med.upenn.edu/microarr). The cRNA targets, generated according to the protocols of the array manufacturer (www.affymetrix.com), were hybridized to the Murine Genome U74 (MG-U74) oligonucleotide array. Absolute and comparison analyses were performed with Affymetrix Microarray Suite 5.0 software. Annotations for all expressed sequence tags (ESTs) were further analyzed with interactive query analysis at www.affymetrix.com and manually with Blast (National Center for Biotechnology Information) to determine the represented genes. The data were filtered for probe sets "present" and increased in wild-type brain RNA with a +2.2-fold or greater change for mRNAs down-regulated in the TB-RBP knockout mice. Similarly, the data were filtered for probe sets "present" and increased in knockout brain RNA with a +2.0-fold or greater change for genes up-regulated in the knockout mice.

Real-time quantitative RT-PCR analysis of representative down-regulated genes. Reverse transcription (RT) of RNA (1 μg) from brains of wild-type and knockout mice was carried out after treatment with amplification-grade DNase I and a RETRO Script RT kit (Ambion, Austin, Tex.). The reverse-transcribed cDNAs were used in triplicate at dilutions of 1:1, 1:10, and 1:100 in a real-time PCR analysis with a model 7700 real-time thermal cycler (ABI, Foster City, Calif.). Primer sets were designed on the basis of 3′ untranslated region sequences for genes analyzed with Primer Express software. Real-time PCR amplification of glyceraldehyde-3-phosphate dehydrogenase was used as a control for normalization. CYBR green reagent (ABI) was used to amplify the genes, and the fold differences were calculated with C_T values.

Antibodies and analytical flow cytometry. Bone marrow (BM), spleen, and thymocyte suspensions were prepared and stained with optimal dilutions of directly conjugated fluorescent antibodies as previously described (24). Antibodies used included fluorescein isothiocyanate-conjugated anti-CD43 (S7), phycoerythrin (PE)-conjugated anti-CD8α (53-6.7), anti-B220 (RA3-6B2), anti-CD19 (1D3), biotin (BI)-conjugated anti-immunoglobulin M (IgM) (R6-60), and allophycocyanin (APC)-conjugated anti-CD4 (RM4-5), anti-AA4 (AA4.1), and anti-T-cell receptor (TcR) β (TcRβ) (H57). All antibodies were purchased from BD Biosciences (Pharmingen Business Unit), San Diego, Calif., except for B220 and AA4 antibodies, which were purified and conjugated by standard methods in our laboratory. BI-conjugated antibodies were revealed with streptavidin-PerCP-Cy5.5 (BD Biosciences), and cells were analyzed on a dual-laser FACScalibur instrument (Becton Dickinson, San Jose, Calif.). The resulting files were uploaded into FlowJo (Tree Star, Inc., San Carlos, Calif.).

Behavioral Rota-Rod testing. Motor coordination was tested with an accelerating Rota-Rod treadmill (manufactured by Ugo Basile and obtained from Stoelting Co., Wood Dale, Ill.), consisting of a 3-cm-diameter rotating rod raised 16 cm above a platform and divided into five sections for testing multiple mice simultaneously. Initially, each mouse was repeatedly placed on the Rota-Rod until it had walked for a total of 30 s at the slowest speed of 4 rpm. After this pretraining, mice were tested three times at 1-h intervals on three consecutive days for a total of nine trials. During each trial, the Rota-Rod was set to accelerate from 4 to 40 rpm over 5 min, and the time at which each mouse fell off the Rota-Rod was recorded with a stopwatch. Fourteen (5 male and 9 female) TB-RBP-null mice and 12 (4 male and 8 female) wild-type littermates between 2 and 4 months old were tested. The mean latency to falling was recorded, and the values were compared between the two groups across the three testing days

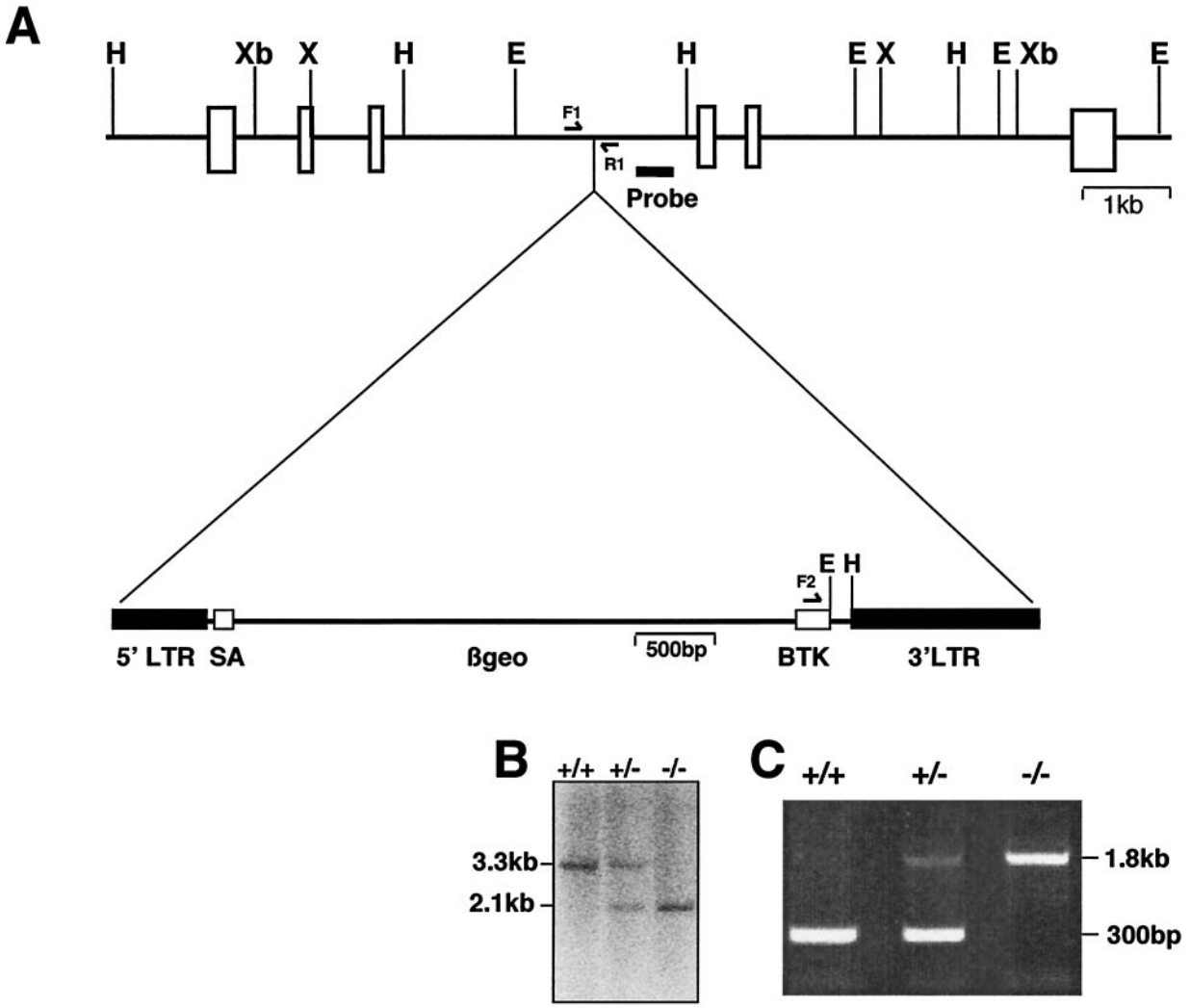

FIG. 1. Targeted mutagenesis of the TB-RBP genomic locus by the gene trap method. (A) Restriction map of the mouse TB-RBP gene showing the six exons and restriction sites (H, *Hin*dIII; Xb, *Xba*I; X, *Xho*I; E, *Eco*RI). The gene trap construct contained a 5′ LTR, a splice acceptor sequence (SA), βgeo, a Bruton tyrosine kinase gene fragment (BTK), and a 3′ LTR. (B) Southern blot of genomic DNA (5 μg) from wild-type, heterozygous, and homozygous targeted mice after restriction digestion with *Hin*dIII. A 400-bp genomic DNA fragment from intron 3 of the TB-RBP gene was used as a probe for the Southern blot analysis. The endogeneous allele is indicated by a 3.3-kb DNA fragment, and the targeted allele is indicated by a 2.1-kb DNA fragment. (C) PCR analysis for genotyping of TB-RBP targeted mice. Genomic DNA samples were PCR amplified with primers F1, F2, and R1 as indicated in panel A. Amplification by primers F1 and R1 gave a 300-bp product from the endogenous allele, whereas primers F2 and R1 amplified a 1.8-kb product from the targeted allele.

by a repeated-measures analysis of variance with trial number, day, and sex as factors.

RESULTS

Generation of TB-RB-deficient mice. Gene trapping was used to generate ES cell clones heterozygous for the TB-RBP mutation. This procedure produced chimeric mice transmitting the mutation into the mouse germ line. The construction of the trapping vector and the production and detection of mutant mice by Southern blot analysis and PCR are described in Fig. 1 and Materials and Methods. The deletion in null animals was detected in Southern blots by the presence of a 2.1-kb DNA fragment following *Hin*dIII digestion (Fig. 1B) or a 1.8-kb amplicon detected by PCR (Fig. 1C).

TB-RBP-deficient mice are viable but stunted at birth. When TB-RBP heterozygotes from the inbred C57BL/6J genetic background were mated, a normal Mendelian ratio of 109 wild-type, 300 heterozygote, and 112 null mice was obtained. Mice heterozygous for TB-RBP were physically indistinguishable from their wild-type littermates. However, birth weights were significantly lower for homozygous TB-RBP mice—10 to 30% lower than the weights of their heterozygous or wild-type littermates (Fig. 2). Concomitant with reduced birth weights, organ weights were proportionately reduced in TB-RBP-null animals, but cell volumes in various tissues were similar among null, heterozygote, and wild-type littermates (data not shown). Histological analyses at the light microscope level of a wide range of organs from 3-month-old mice (brain, lungs, heart,

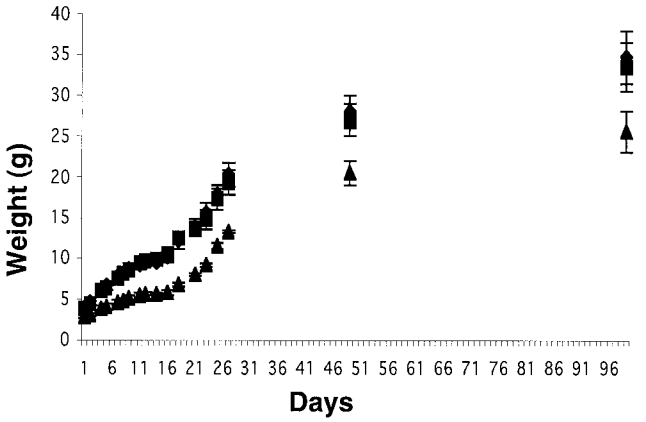

FIG. 2. Growth curves for a representative litter from a heterozygous cross showing that +/+ (squares) and ± (triangles) mice have similar growth rates (upper curve), while −/− mice (lower curve) have a lower growth rate from birth to 96 days after birth. By 6 months of age, no significant difference in weight was seen between null mice and their littermates. Data are means and SEMs.

liver, spleen, kidneys, epididymis, ovaries, eyes, uterus, adrenal glands, stomach, and intestines) showed normal morphology.

Although birth weights and weight at 1 month of age were significantly lower in TB-RBP-null mice than in their heterozygous or wild-type littermates, by 6 months of age, there was no difference in weights among the three groups. To determine the component of body mass responsible for this catching up in growth, body composition analysis was measured by use of DEXA. At the time of the study, animals were 5 to 6 months old. The percentage of total fat mass was significantly increased in null animals, averaging 32.38% ± 2.37% (mean and SEM); values for heterozygous and wild-type littermates were 18.17% ± 2.01% and 6.55% ± 0.46%, respectively. In contrast, lean body mass was significantly decreased in null animals compared with heterozygous and wild-type littermates (21.56 ± 1.55 [mean and SEM], 28.13 ± 0.90, and 25.28 ± 1.25 g, respectively). Lengths were also reduced in null mice compared with heterozygous and wild-type littermates (9.1, 9.5, and 9.7 cm, respectively); however, bone densities were similar among the three groups. Null mice had a disproportionate accumulation of fat mass in the abdominal region, defined as the area between the lower border of the thoracic rib cage and the upper border of the pelvic cavity. This region contains several fat depots, including visceral, retroperitoneal, and surrounding subcutaneous fat.

Since the TB-RBP-null mice were smaller at birth, we investigated cell proliferation in embryos by labeling mouse embryos at 14.5 days of gestation with bromodeoxyuridine. When two representative organs, the kidneys and lungs, were analyzed, reduced cellular proliferation was seen in TB-RBP-null animals compared to their littermates, consistent with the reduced organ weights and reduced animal weights at birth (data not shown).

TB-RBP and its interacting protein, TRAX, are absent in TB-RBP-deficient mice. To confirm that the gene trapping of TB-RBP functionally deleted TB-RBP expression, Western blots of protein extracts of brain, heart, kidneys, liver, lungs, spleen, and testes were assayed for TB-RBP with an affinity-purified antibody (40). No TB-RBP was detected in extracts prepared from homozygous null mice, whereas the level of TB-RBP from heterozygote extracts was approximately 50% that from wild-type extracts (Fig. 3A). Similar reductions in the levels of the related and TB-RBP-interacting protein TRAX were seen in extracts from heterozygous and homozygous mice (Fig. 3A), suggesting a coordinated loss of steady-state levels of TB-RBP and TRAX. There was no reduction in the levels of the control proteins, actin and tubulin (data not shown).

To determine whether the reduction in and loss of TRAX in heterozygous and homozygous mice, respectively, were regulated at transcriptional or posttranscriptional levels, Northern blots were prepared with total RNAs from the brains, lungs, and testes from wild-type, heterozygous, and homozygous mice. The TB-RBP mRNA levels reflected allelic numbers, with about a 50% reduction in the heterozygous mice and no detectable TB-RBP mRNA in the homozygous mice (Fig. 3B). No differences in TRAX mRNA levels were detected in the wild-type, heterozygous, and null animals, suggesting that the reduction in TRAX reflected a posttranscriptional loss, perhaps directly caused by the deficiency of TB-RBP.

B- and T-cell development is normal in the absence of TB-RBP. Given the proposed role of Translin/TB-RBP in processes required for early lymphocyte development, such as immunoglobulin or TcR rearrangements (6), we tested whether the targeted deletion of TB-RBP had a negative impact on early T- and B-cell development. In the thymus, early T-cell precursors are defined by a lack of cell surface expression of the coreceptor molecules CD4 and CD8. These $CD4^-$ $CD8^-$ cells are often termed double-negative (DN) thymocytes, and productive recombination of the TcRβ locus in these cells is required for their differentiation into $CD4^+$ $CD8^+$ double-positive (DP) thymocytes. The latter are further characterized by additional rearrangements in the TcRα locus and, upon synthesis of TcRα-TcRβ heterodimers, subsequent selection and differentiation into $CD4^+$ $CD8^-$ or $CD4^-$ $CD8^+$ single-positive (SP) T cells (30, 53). We reasoned that if TB-RBP played a requisite function in V(D)J recombination of TcR loci in mice, then T-cell development in null mice would be arrested at the DN stage in a manner similar to that in V(D)J recombinase-activating gene (Rag)-deficient mice (39, 47). However, wild-type and null mice had equivalent percentages and absolute numbers of DN, DP, and SP (both types) thymocytes (Fig. 4, left-most panels), suggesting that TB-RBP activity is not required for efficient T-cell development.

In BM, analogous V(D)J rearrangement events of the immunoglobulin heavy-chain locus are required for CD45R/$B220^+$ $CD43^+$ pro-B cells to differentiate into CD45R/$B220^+$ $CD43^-$ $AA4^+$ secretory IgM-negative pre-B cells (reviewed in reference 20). Moreover, recombination of immunoglobulin light-chain loci are required for the differentiation of pre-B cells into newly formed $AA4^+$ secretory IgM-positive BM B cells (1). We were also unable to detect differences in the representations of these B-cell populations in BM of wild-type or null mice (Fig. 4, two sets of center panels). Finally, while null mice had marginally reduced numbers of splenocytes, the percentages of $CD19^+$ B cells and TcRβ-positive T cells were comparable in wild-type and null mice (Fig. 4, right-most panels). Collectively, these data indicate that TB-RBP activity is not essential for normal B- and T-cell development.

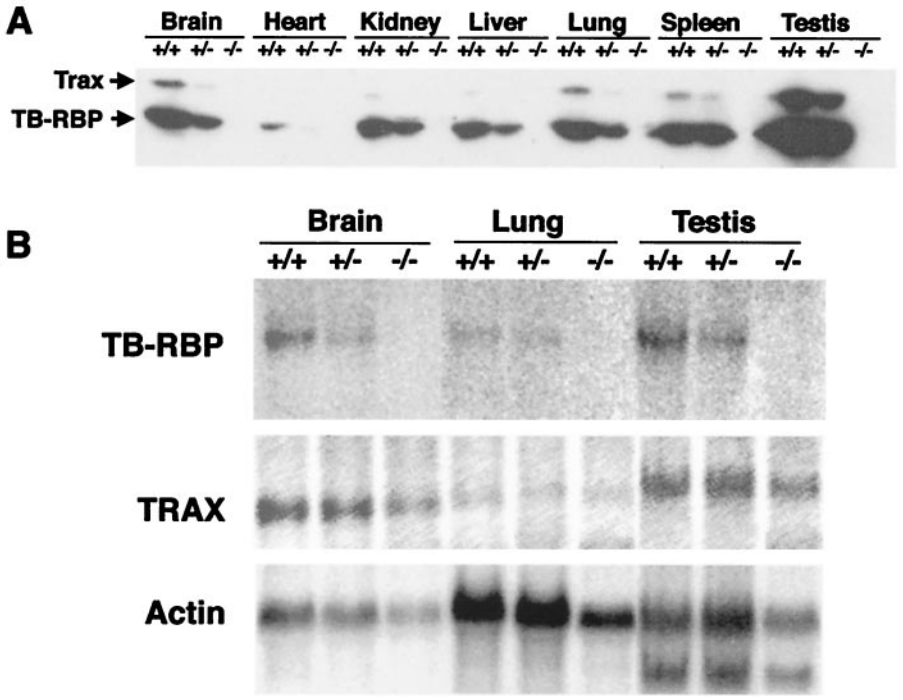

FIG. 3. Distributions of TB-RBP and TRAX and of their mRNAs in mouse tissues. (A) Western blot of TB-RBP and TRAX in various tissues of +/+, +/−, and −/− mice. Postmitochondrial extracts (30 μg) from adult mice were separated by SDS–10% polyacrylamide gel electrophoresis, transferred to nylon membranes, and probed with affinity-purified antibodies to TB-RBP and TRAX. To detect any residual TB-RBP in extracts from null mice, the Western blot was intentionally overexposed. (B) Northern blot analysis of TB-RBP and TRAX mRNAs in brains, lung, and testes of +/+, +/−, and −/− mice. Total RNAs (10 μg) from adult mice were hybridized to cDNAs encoding TB-RBP, TRAX, and actin.

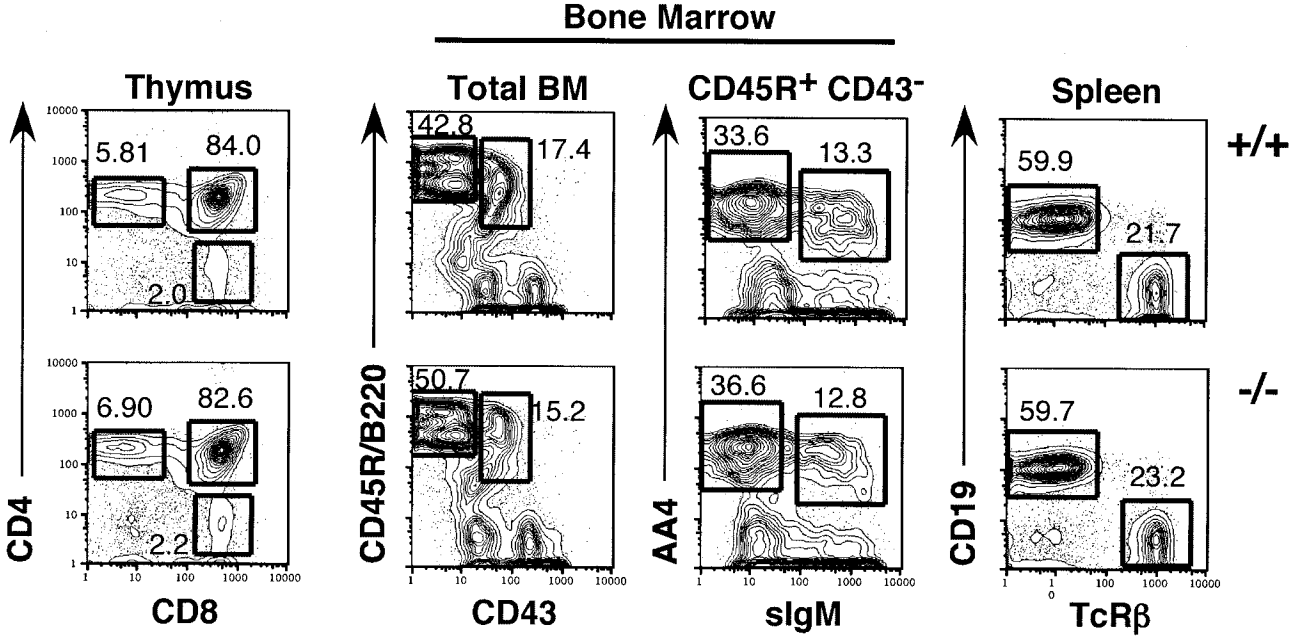

FIG. 4. Normal T- and B-cell development in TB-RBP-deficient adult mice. Thymocytes, BM cells, and splenocytes from null and wild-type littermate controls were stained as follows. Thymocytes were stained with PE–anti-CD8 and APC–anti-CD4; BM cells were stained with fluorescein isothiocyanate–anti-CD43, PE–anti-B220, BI–anti-IgM, and APC–anti-AA4; and splenocytes were stained with PE–anti-CD19 and APC–anti-TcRβ. A total of 100,000 cells/tube were analyzed by flow cytometry as described in Materials and Methods. Numbers indicate percentages of total cells. sIgM, secretory IgM.

TABLE 1. Diminished sperm production in TB-RBP-null animals[a]

Age (mo)	Genotype	Testis wt, g	No. of spermatozoa, 10^6/ml
2	+/+ or +/−	0.20 ± 0.03 (10)	21.15 ± 1.76 (10)
	−/−	0.16 ± 0.02 (8)	11.2 ± 4.5 (8)
3	+/−	0.215 ± 0.015 (2)	28.0 ± 0 (2)
	−/−	0.168 ± 0.035 (4)	16.6 ± 8.4 (4)
7	+/−	0.24 ± 0.04 (4)	36.71 ± 7.59 (4)
	−/−	0.18 ± 0.010 (4)	14.36 ± 3.54 (4)
9	+/−	0.175 ± 0.025 (2)	37.51 ± 3.74 (2)
	−/−	0.18 ± 0.01 (2)	11.9 ± 2.4 (2)

[a] Data are reported as means and standard errors of means (number of mice tested).

FSH and LH levels and seminal vesicle weights are normal in TB-RBP-deficient mice. Serum FSH and LH levels were measured by radioimmunoassays of samples from the blood of null males and their wild-type and heterozygous male littermates. FSH levels were slightly higher in null males (46.07 ± 15.37 ng/ml [mean and SEM]; $n = 14$) than in their wild-type (39 ± 5.48 ng/ml; $n = 4$) or heterozygous (41 ± 9.24 ng/ml; $n = 10$) male littermates. LH levels were slightly lower in null males (0.25 ± 0.10 ng/ml; $n = 11$) than in their wild-type (0.25 ± 0.05 ng/ml; $n = 4$) or heterozygous (0.29 ± 0.16 ng/ml; $n = 9$) male littermates. Seminal vesicle weights were somewhat lower in null males (0.23 ± 0.04 g [mean and SEM]; $n = 4$) than in their wild-type or heterozygous littermates (0.28 ± 0.03 g; $n = 6$), a decrease proportional to that seen in testis weights (0.21 ± 0.02 versus 0.16 ± 0.01 g). None of the differences in FSH, LH, or seminal vesicle weights were statistically significant.

TB-RBP-null males are fertile but produce fewer spermatozoa and show abnormal spermatogenesis. To examine the fertility of TB-RBP-null mice, homozygous males and females were bred to wild-type or heterozygous animals. Null males were fertile, and males up to 13 months old (not tested longer) sired offspring, producing litters of the same size (eight or nine pups/litter) and frequency as their wild-type male littermates. However, despite normal fertility, sperm counts were consistently lower in null mice—about one-third those in their littermates—for 9-month-old mice (Table 1). Reduced numbers of sperm were seen in null mice as young as 43 days (data not shown), and the reduction in sperm counts in null mice and their littermates appeared to increase with age. No significant differences were detected in the motility of null, heterozygote, and wild-type spermatozoa or in epididymal weights.

Seminiferous tubules appeared mostly normal in 2-month-old null male mice, although there were vacuoles in small regions (Fig. 5D and E, arrows). Vacuolization appeared to progress with age and was much more widespread in older null male mice (Fig. 5J and K). In contrast, no vacuoles were seen in wild-type littermates (Fig. 5A, B, G, and H). Interestingly, males 6 to 8 months old occasionally showed no abnormal morphology in the testes. Despite substantial seminiferous tubule degeneration, virtually all of the null male mice were able to sire litters.

In testes from wild-type mice, TB-RBP is abundant in meiotic pachytene spermatocyte nuclei and in the cytoplasm of the subsequent stages of meiotic and postmeiotic germ cells (Fig. 5A, inset). To determine the cell types that are the first to be lost in null mice, TUNEL assays were performed (Fig. 5). There was a significant increase in the number of TUNEL-positive cells from primarily pachytene spermatocytes to metaphase 1 (Fig. 5L, inset) in 2-month-old mice, the age when seminiferous tubules begin to show abnormalities. By 8 months of age, there were far fewer TUNEL-positive cells in the heavily vacuolated tubules, suggesting that cell death preceded vacuolization.

Null females produce fewer and smaller litters. The fertility of null females was significantly reduced compared to that of their heterozygous or wild-type littermates. When mated with experienced heterozygous or wild-type males, null females averaged 68.8 ± 2.2 days between litters, while control matings averaged 32.2 ± 2.2 days between litters. The litter sizes of null females were also reduced, averaging four pups, compared to eight pups for their heterozygous littermates. Preliminary histological analyses revealed no obvious defects in the reproductive tracts of the null females, and the cause(s) of the reduced fertility is under investigation.

TB-RBP ablation leads to altered gene expression in the brains of null mice. Since TB-RBP and its associated protein, TRAX, are abundant in the brain and an association between TB-RBP and transported mRNAs has been demonstrated in neuronal cells (17, 28, 46), we examined the influence of the TB-RBP-null mutation on the overall gene transcription profile in adult mouse brains by using MG-U74 oligonucleotide array hybridization. The MG-U74 chip contains 12,473 probe sets.

DNA microarray analysis of pooled RNAs from the brains of wild-type and TB-RBP-null mice showed significant differences in gene expression (Tables 2 and 3). Hybridizing mRNAs, corresponding to 4,868 probe sets (39%), were detected in the brain samples. With a fold difference cutoff of 2.2, 217 (4.46%) of the genes were down-regulated in the brains of null mice compared to the brains of wild-type mice. The down-regulated genes were clustered manually into groups based on their biochemical and cellular functions inferred from published data related to those genes and/or gene names. Prominent among genes significantly down-regulated in the brains of null mice were those for neurotransmitter receptors (subunits of the glutamate receptor and the γ-aminobutyric acid A [GABA-A] receptor) (Table 2, neurotransmitter receptors and ion channels) and vesicle sorting and transport proteins (synaptobrevin-like protein and VPS41) (Table 2, vesicle sorting and transport). Genes for nucleic acid-binding proteins and transcription factors, such as glucocorticoid receptor 1, accounted for a significant portion of the down-regulated genes (Table 2, nucleic acid-binding proteins and transcription factors). A number of cell cycle-related genes, including those for cyclin E2 and cyclin C, showed major (15-fold) decreases in brains from null animals (Table 2, cell cycle and apoptosis). Significant decreases were also found in mRNAs involved in G protein signaling (p190-B; Table 2, G protein signaling), growth factors (growth hormone, fibroblast growth factor 12, prolactin, and mast cell growth factor; Table 2, growth hormones and growth factors), cellular metabolism proteins (folate hydrolase and α-1,3-fucosyltransferase; Table 2, metabolic

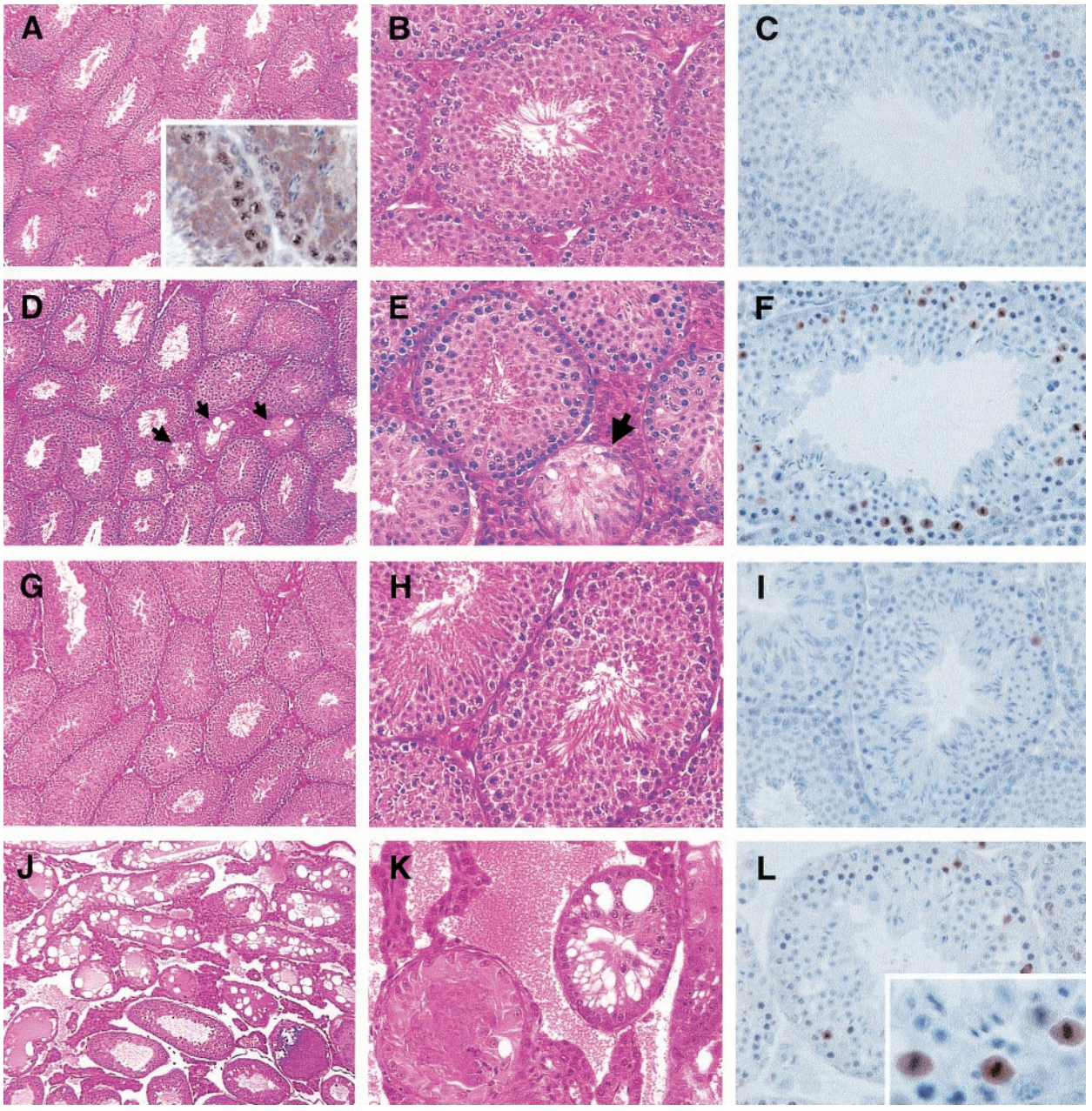

FIG. 5. Testes from null mice show abnormal spermatogenesis and increased cell death. Histological analysis of Bouin fixative-fixed testicular sections from wild-type mice (A to C and G to I) and TB-RBP-null mice (D to F and J to L) that were 2 months old (A to F) and 8 months old (G to L) is shown. Samples in panels A, B, D, E, G, H, J, and K were stained with hematoxylin and eosin. Samples in panels C, F, I, and L were stained with an ApopTag peroxidase staining kit and counterstained with hematoxylin. Arrows in panels D and E show vacuoles. The inset in panel A shows the immunolocalization of TB-RBP in testes from wild-type mice by use of an affinity-purified antibody to TB-RBP and horseradish peroxidase staining. The inset in panel L shows meiosis-arrested germ cells undergoing cell death. Magnifications: A, D, G, and J, ×25; B, C, E, F, H, I, K, and L, ×100.

and biosynthetic enzymes), the cytoskeletal protein MAP-2 (Table 2, cytoskeleton-associated proteins), kinases and phosphatases (a subunit of the phosphatidylinositol 3-kinase and protein tyrosine phosphatase receptor type D; Table 2, kinases and phosphatases), several neuronal growth and differentiation factors (including myelin proteolipid protein and a DSD-1 proteoglycan; Table 2, neuronal growth and differentiation), and miscellaneous proteins (such as nuclear matrix protein and matrin 3; Table 2, additional proteins).

To validate the microarray results, real-time RT-PCR assays were performed with four representative mRNAs that showed major down-regulation in the microarray analysis (glutamate receptor α3 subunit, GABA-A receptor α1 subunit, a synaptobrevin-like protein, and MAP-2). Real-time RT-PCR assays

TABLE 2. Cluster analysis of genes down-regulated in brains of null mice[a]

Category	Accession no.	Protein	Fold decrease	Proposed function(s)
Neurotransmitter receptors and ion channels	AB022342	Glutamate receptor channel α3 subunit	18.0	
	X61430	GABA-A receptor α1 subunit	7.9	
	L42339	*Mus musculus* sodium channel 3	4.1	
	X57498	Glutamate receptor, ionotropic, AMPA2 (α2)	3.2	
	X78874	Chloride channel 3	3.2	
	X51986	GABA-A receptor α6 subunit	3.0	
	X57349	Transferrin receptor	3.0	
	D50086	Neuropilin	3.0	
	AI839615	K^+ voltage-gated channel, Sha1 related, member 2	2.7	
	X78667	Ryr2	2.4	
	AW061228	ATPase, Ca^{2+} transporting, type 2C	2.4	
	M30440	K^+ voltage-gated channel, Shaker related 2	2.3	
	U88623	Aquaporin 4	2.3	
	AI594427	Sodium bicarbonate cotransporter	2.3	
Vesicle sorting and transport	X96737	Synaptobrevin-like protein	24	
	A1848222	Vacuolar protein sorting VPS41	14	
	D29797	Syntaxin 3A	5.4	
	AI850801	Similar to coated vesicle membrane protein	2.7	
	AI845514	ABCA1	3.6	
	U13174	Solute carrier family 12, member 2	3.4	
	U04827	Brain fatty acid-binding protein	2.6	
	D50032	TGN38B	2.4	
Nucleic acid-binding proteins	M36514	Mouse zinc finger protein (mkr3) mRNA	16	
	AJ237846	hnRNP G, splice variant 2	6.4	
	AI551105	midline 2 (Mid2), zinc finger protein	5.6	
	AB024005	KRAB-containing zinc finger protein KRAZ2	4.4	
	L36316	Zinc finger protein 63	3.6	
	AI835041	Zinc finger protein 265 putative orthologue	3.6	
	AI842878	46-kDa arginine/serine-rich splicing factor, SRP46	3.5	
	L23971	Fragile X mental retardation syndrome 1 homologue	3.4	
	AF038939	Zinc finger protein (Peg3) mRNA	3.4	
	X07699	Nucleolin	3.2	
	L25126	DEAD box polypeptide 3	3.1	
	AJ007376	DBY RNA helicase	2.9	
	U29088	Human antigen D	2.9	
	AB020542	Zinc finger protein s11-6	2.9	
	AV299153	DEAD/DEAH box helicase	2.8	
	AW049372	Splicing factor 3b, subunit 1, 155 kDa	2.8	
	AA866971	Nucleolar RNA helicase GU2	2.7	
	Y15907	Myc intron-binding protein 1	2.6	
	L20450	DNA-binding protein mRNA, zinc finger protein	2.6	
	AJ132922	Methyl-CpG-binding protein 2	2.5	
	AI646981	AKAP95	2.5	
	AW226540	GA repeat-binding protein α	2.5	
	U48721	Zinc finger protein 62	2.5	
	AI846392	NS1-associated protein 1	2.4	
	D38046	Type II DNA topoisomerase β isoform	2.4	
	U18773	GPI-anchored protein p137	2.4	
	AW046194	Similar to hnRNP A3	2.4	
	AF037205	RING zinc finger protein (Rzf) mRNA	2.4	
	AB024004	KRAB-containing zinc finger protein KRAZ1	2.3	
	AI838709	Spermatid perinuclear RNA-binding protein	2.3	
	X90875	FXR1 protein	2.3	
	Z67747	ZT3 zinc finger factor	2.3	
	M64068	Zinc finger protein (bmi-1)	2.3	
	AA795486	Human immunodeficiency virus type 1 Rev-binding protein, Hrb	2.3	
	Y14196	hnRNP H	2.2	
	X65627	DEAD box polypeptide 5	2.2	
	AI846060	Zinc finger RNA-binding protein	2.2	
	AA688834	RNP1- and RRM-containing protein	2.2	

Continued on following page

TABLE 2—*Continued*

Category	Accession no.	Protein	Fold decrease	Proposed function(s)
Transcription factors	X04435	Glucocorticoid receptor 1	7.9	
	AI595996	Myocyte enhancer factor, Mef2c	7.8	
	Y14296	BTEB-1 transcription factor	4.1	
	U53228	Retinoic acid receptor-related orphan receptor α	4.1	
	AI848888	Elongation factor SIII p15 subunit, Skp1 family	3.9	
	U09504	Thyroid hormone receptor α	3.7	
	AA759910	Transcription factor e(y)2	3.6	
	Y09085	Hypoxia-inducible factor 1, α subunit	3.1	
	U61363	Groucho-related gene 4 (Grg4)	3.1	
	AI098965	Transcription repressor protein GCF	3.1	
	AW107230	Nucleosome assembly protein 1-like protein	3.0	
	AI848062	Myelin transcription factor 1-like protein	2.9	
	D00925	Transcription factor SII-related protein	2.6	
	U46026	Activating transcription factor 2	2.6	
	AF062567	Transcription factor Sp3	2.6	
	AI197161	ELL-related RNA polymerase II, elongation factor	2.6	
	AW124932	Pre-B-cell leukemia transcription factor 1	2.5	
	AI848056	Eukaryotic translation initiation factor 3, subunit 1	2.4	
	D76432	Transcription factor 8	2.2	
G protein signaling	U67160	p190-B	18	
	AI194333	Rab-GTPase-activating protein	3.8	
	AA958696	Regulator of G protein signaling 5	3.7	
	AI841377	RAB5A	2.7	
	U38501	Guanine nucleotide binding, α inhibiting	2.5	
	AA763874	ARF6-interacting protein 2	2.3	
	U67187	G protein signaling regulator RGS2 (rgs2)	2.2	
Cell cycle and apoptosis	AI626975	Cyclin E2	15	
	U62638	Cyclin C	15	
	AI840051	Cullin 3	4.5	
	AJ223782	CDC10	4	
	M38381	CDC-like kinase	3.1	
	AI845038	Tousled-like kinase 2	2.9	
	U88909	Apoptosis inhibitor 2	2.8	
	AW124633b	NIMA (never in mitosis gene A)-related kinase 7	2.4	
	D86344	Topoisomerase inhibitor suppressed	2.4	
	U39074	Thymopoietin	2.2	
	AI846393	APP-binding protein 1	2.2	
Growth hormones and growth factors	X02891	Growth hormone	17	
	U66201	Fibroblast growth factor 12	5.2	
	AI852144	Pre-B-cell colony-enhancing factor	4.8	
	X04418	Prolactin	4.4	
	AW124983	Epidermal growth factor receptor pathway substrate 15, Eps15	4.3	
	AI851595	Inhibin β c	4.0	
	M57647	Mast cell growth factor	3.9	
	J00643	Glycoprotein hormones, α subunit	3.5	
Metabolic and biosynthetic enzymes	AA986395	Folate hydrolase	30	
	AB015426	α-1,3-Fucosyltransferase IX (Fut9)	14	
	U48896	UDP-glucuronosyltransferase 8	4.7	
	AA619207	Fatty acid coenzyme A ligase	4.1	
	J00356	Mouse α-amylase 1	4.0	
	L42996	Nucleus-encoded mitochondrial acyltransferase	4.2	
	U95116	Platelet-activating factor acetylhydrolase 1b, β1	3.2	
	D89866	Ceramide glucosyltransferase	3.1	
	AA734806	*N*-Arginine dibasic convertase 1	2.7	
	AW125314	UDP-Gal:βGlcNAc β-1,4-galactosyltransferase	2.3	
Cytoskeleton-associated proteins	M21041	Microtubule-associated protein 2	6.6	
	U16741	Capping protein α 2	3.5	
	AF067180	Kinesin heavy-chain member 5C	3.0	
	D12644	Kinesin heavy-chain member 2	2.7	
	L29468	Cofilin isoform	2.5	
	D50367	KAP3B	2.4	

Continued on following page

TABLE 2—*Continued*

Category	Accession no.	Protein	Fold decrease	Proposed function(s)
Kinases and phosphatases	AW121773	Phosphatidylinositol 3-kinase α subunit	18	
	D13903	Protein tyrosine phosphatase, receptor type D	5.4	
	AI849305	Tyrosine phosphatase, receptor type Z1	4.3	
	AF096285	Serine/threonine kinase receptor-associated protein	4.2	
	AW124985	Nuclear autoantigen similar to striatin	3.1	
	M27073	Protein phosphatase 1, catalytic subunit	2.8	
	AI848984	Phosphatase and tensin homologue	2.5	
	AW124934	Pellino 1	2.5	
	AI852314	Protein phosphatase 4 regulatory subunit 2	2.4	
Neuronal growth and differentiation	M37335	Myelin proteolipid protein	4.2	
	X94310	L1-like protein	3.6	
	AJ133130	DSD-1-proteoglycan	3.5	
	U42386	Fibroblast growth factor inducible gene 14	3.3	
	L25274	Transmembrane glycoprotein (DM-GRASP)	3.0	
	AJ001700	Neuroserpin	2.9	
	AI843178	Cerebellar postnatal development protein 1	2.7	
	AF051357	Golgin-245 (olp-1)	2.3	
Additional proteins	AB009275	Matrin 3	7.9	Nuclear matrix structural protein
	AI844238	SUMO-1-specific protease SUS1	6.1	Protein turnover
	AW124175	Sarcolemmal-associated protein	5.8	Duchenne muscular dystrophy
	AW046889	Similar to midasin (yeast)	3.9	AAA ATPase, Nuclear chaperone
	AI836959	ADAMS homologue	3.8	Neuroinflammation
	D50523	TI-227	3.4	Cancer metastasis-associated protein
	AF020771	Importin α Q1	3.2	Nuclear localization sequence receptor
	AB014464	MGC-24v	3.0	Glycoprotein, hematopoiesis
	U73039	Next to Brcal	3.0	signaling
	AI836686	Calcium-binding protein, Mo25	2.9	Morula, Ca binding
	X61455	I47	2.9	Unknown
	U56724	Dystrophin	2.8	DMD, cytoskeletal function
	AW120783	Ankyrin repeat	2.8	Various roles
	AB008516	Tetratricopeptide repeat	2.7	Interaction with heat shock protein
	U90446	RNase L inhibitor (Mu-RLI)	2.5	Viral infection, defense
	U96760	VHL-binding protein (vbp-1)	2.4	Cullin association, ubiquitination
	AI835367	Matrin 3 homologue	2.4	Nuclear matrix structural protein
	U42384	Fibroblast growth factor inducible gene 15	2.4	Signaling
	X15202	Fibronectin receptor β (VLA5)	2.3	Integrin
	AF033186	WSB-1	2.3	Suppressor of cytokine signaling
	AF061260	Immunosuperfamily protein B12	2.3	Immunity
	AA882416	Translocation protein 1	2.2	Protein translocation, endoplasmic reticulum
ESTs	AA543502		32.5	
	AW122483		28.7	
	AI573367		15.1	
	AW011716		11.2	
	AI843267		11	
	AW047929		9.4	
	AA693125		9.1	
	AI648965		5.4	
ESTs	AA543502		32.5	
	AW122483		28.7	
	AI573367		15.1	
	AW011716		11.2	

Continued on following page

TABLE 2—*Continued*

Category	Accession no.	Protein	Fold decrease	Proposed function(s)
	AI843267		11	
	AW047929		9.4	
	AA693125		9.1	
	AI648965		5.4	
	AI194254		4.9	
	AA690483		4	
	AI848671		3.9	
	AW060250		3.8	
	AA867655		3.7	
	AI844911		3.5	
	AI845607		3.5	
	AW122573		3.5	
	AI465845		3.5	
	AW260482		3.4	
	AI848330		3.4	
	AI837467		3.3	
	AA717740		3.3	
	AW060212		3.2	
	AA543502		3.2	
	AI842065		3.2	
	AW122450		3.2	
	AW123269		3.2	
	AI850675		3.1	
	AA666464		3	
	AA189811		2.9	
	AW047329		2.9	
	AW046160		2.9	
	AA866655		2.9	
	AI788669		2.8	
	AI854214		2.8	
	AA693236		2.7	
	C76063		2.7	
	AW122195		2.7	
	AI852916		2.6	
	AA163268		2.5	
	AI854118		2.5	
	AW107884		2.4	
	AI842264		2.4	
	AA755234		2.4	
	AI852287		2.4	
	AI746846		2.4	
	AW120676		2.4	
	AA122571		2.4	
	AW121745		2.3	
	AI839117		2.3	
	AW047331		2.3	
	AA592069		2.2	
	AA823202		2.2	
	AW228840		2.2	
	AI225869		2.2	
	AI846896		2.2	

[a] DBY, Dead box protein y; GPI, glycosyl phosphatidyl inositol; RRM, RNA recognition motif; APP, amyloid precursor protein; DSD, depression spectrum disease.

confirmed the microarray results and in fact revealed that the mRNA fold decreases determined by the microarray analysis were actually underestimates (Table 3). Fold changes were calculated after the respective C_T values were normalized to that of glyceraldehyde-3-phosphate dehydrogenase mRNA.

Since decreases in mRNA levels do not always lead to equivalent decreases in protein levels, Western blotting analyses were used to measure the levels of two proteins, MAP-2 and GABA-A receptor α1, encoded by mRNAs down-regulated in the brains of null mice (Table 2). MAP-2 levels were decreased 8-fold in protein extracts from total brain and GABA-A re-

TABLE 3. Real-time RT-PCR confirmation of down-regulation of four mRNAs

Gene	Fold decrease determined by the following analysis:	
	Microarray	RT-PCR
Glutamate receptor α3	18.0	56
GABA-A receptor α1	7.9	6.5
Synaptobrevin-like protein	24.0	28
MAP-2	6.6	19.7

TABLE 4. Genes up-regulated in brains of null mice

Accession no.	Protein	Fold increase
AV316991	EST	6.5
M90551	Intercellular adhesion molecule	4.3
AV207158	EST	3.9
M99492	Butyrylocholinesterase	3.8
U79523	peptidylglycine α-amidating monooxygenase	3.3
C79288	EST	2.6
AV321289	Heat-responsive protein 12; translation inhibitor p14.5	2.5
AA989957	SMAF1	2.3
D64162	Rae123 cell surface protein	2.3
X57638	Peroxisome proliferator-activated receptor α	2.3
AV218205	Cystatin 3	2.1
AA016517	Mac-2-binding glycoprotein precursor	2.0
AJ005564	Small proline-rich protein 2F	2.0
AV100072	Superoxide dismutase 1, soluble	2.0

ceptor α1 levels were decreased 20-fold in protein extracts from microsomal preparations in TB-RBP-null mice.

Although inhibition of TB-RBP leads to a major down-regulation of gene expression in the brain, a few (14) mRNAs were up-regulated in null animals compared to wild-type animals (on the basis of a criterion of 2.0-fold or greater) (Table 4). Among the identifiable up-regulated genes, the genes for an intercellular adhesion molecule and butyrylcholinesterase were increased 4.3- and 3.8-fold, respectively.

Inhibition of TB-RBP leads to behavioral defects in null mice. Figure 6 shows the performance of TB-RBP-null mice and wild-type littermates on the accelerating Rota-Rod over nine trials. The Rota-Rod is used to test the cerebellum-dependent functions of balance, coordination, and motor learning. It also measures endurance and muscle grip strength. As a group, TB-RBP-deficient mice consistently fell from the Rota-Rod sooner than wild-type controls. There was a significant effect of genotype on the mean latency to falling from the rotating rod ($F_{1,22} = 9.231$, $P < 0.01$). Despite the decreased performance of the null mice, both groups improved significantly across trials ($F_{8,176} = 16.306$, $P < 0.001$). There was no interaction between trial and genotype ($F_{8,176} = 0.877$, $P = 0.537$), indicating that the rates of improvement did not differ significantly between the null animals and their wild-type littermates. There was no significant effect of sex on Rota-Rod performance, and so males and females were considered together. Given the reduced weights of the TB-RBP-null mice, we were concerned that the decreased performance on the Rota-Rod might be related to their smaller sizes. However, when body weight was included as a covariate, there was still a significant effect of genotype on Rota-Rod performance ($F_{1,21} = 15.670$, $P = 0.001$).

DISCUSSION

The complex phenotype exhibited by TB-RBP-deficient mice likely reflects the multiple functions of TB-RBP as a DNA, RNA, and microtubule-binding protein. The human orthologue, Translin, was originally identified as a protein that specifically binds to consensus sequences at breakpoint junc-

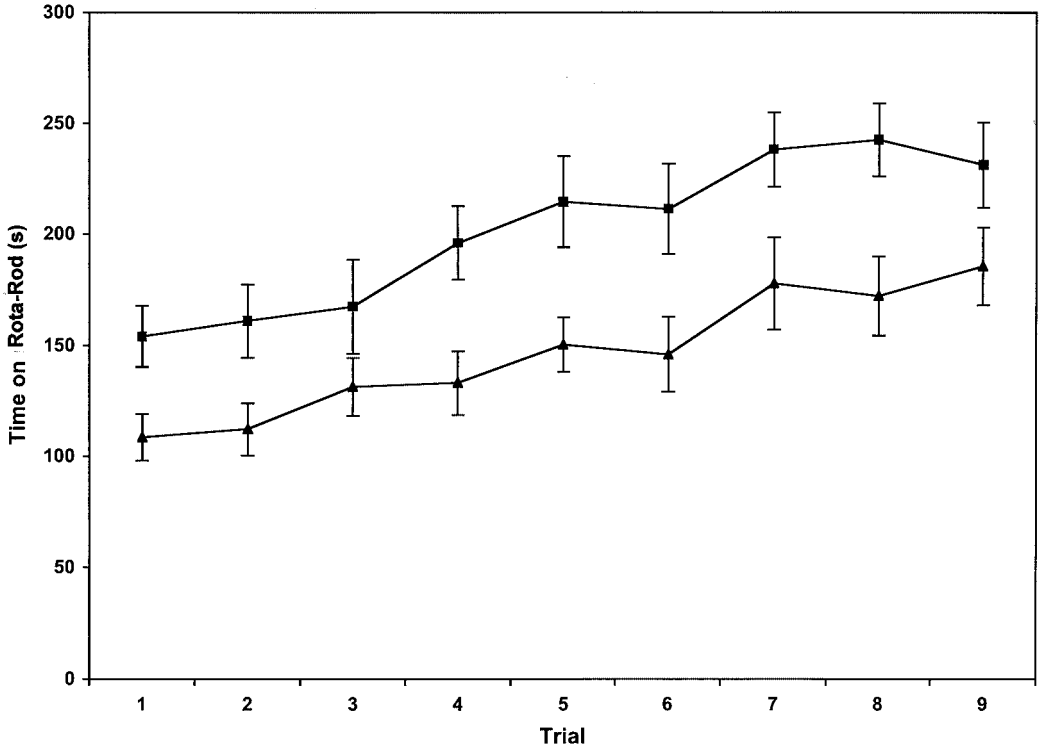

FIG. 6. Disruption of TB-RBP leads to behavioral deficits in the accelerating Rota-Rod test. The latency to falling (mean and SEM) for TB-RBP knockout mice (▲) was significantly shorter than that for wild-type littermates (■) over nine trials. The performance of both groups improved significantly over the course of training, but the rates of improvement did not differ significantly.

tions of chromosomal translocations in many lymphoid malignancies (6). The direct relationship among Translin protein level, the proliferative state of cells (22), and the growth retardation resulting from TB-RBP deficiency (Fig. 2) suggests that Translin/TB-RBP can also influence the cell cycle. Translin binds both γ-tubulin and α-tubulin (22), consistent with a role for this protein in microtubule organization, stabilization, and/or chromosome segregation during mitosis. TB-RBP has been shown to link specific mRNAs to microtubules (19, 32, 59). The binding of TB-RBP to microtubules and actin would allow cytoskeletal TB-RBP-mediated mRNA transport. In the germ cells of the mouse testis, TB-RBP and the Ter ATPase form complexes with specific mRNAs as the mRNAs are transported from the nucleus to the cytoplasm and through the intercellular bridges connecting the germ cells in a syncytium (22). A testicular motor protein that binds to a TB-RBP–mRNA complex which may facilitate its movement was recently identified (V. Chennathukuzhi and N. B. Hecht, unpublished data).

The complex phenotype of the null animals may also indicate different tissue-specific functions for TB-RBP. Using an affinity-purified antibody for immunohistochemical analysis and Western blotting, we found TB-RBP to be widely expressed in embryos (data not shown) and ubiquitously expressed in adult mice, but at vastly different levels (Fig. 3). High levels in liver of microRNAs that are bound to TB-RBP, preventing its binding to RNA probes in gel shift assays, were recently found (T. D. Raabe and N. B. Hecht, unpublished data). This finding may explain the observations that TB-RBP in extracts from testis and brain binds strongly to RNA gel shift probes but that TB-RBP in other somatic cell extracts does not (18). This apparent diminished binding of TB-RBP is due to endogeneous RNA binding to TB-RBP in somatic cells (16). The regulatory function, if any, of these TB-RBP–microRNA complexes in organs such as the liver remains to be determined. Similar protein-microRNA complexes containing another RNA-binding protein, the fragile X syndrome protein, have been reported (11, 23).

Interactions with different proteins may also influence TB-RBP function. A complex of TB-RBP and a transport ATPase, the Ter ATPase, accompanies specific mRNAs through nuclear pores and intercellular bridges (41). The protein with the most extensive amino acid homology to Translin, TRAX, forms complexes with Translin/TB-RBP (12, 17). In the brain, TB-RBP alone or in association with TRAX is involved in the somato-dendritic sorting of mRNAs (17, 28). DNA damage has been demonstrated to selectively induce interactions of TRAX with the nuclear matrix protein, C1D, an activator of the DNA-dependent protein kinase, supporting a role for TRAX independent of TB-RBP in the repair of double-stranded DNA and V(D)J recombination (14, 15).

Based on the numerous possible functions of TB-RBP, some of the phenotypes exhibited by the null mice were predictable, while others were surprising. The reduced size of the null mice at birth strongly supports the hypothesis that Translin/TB-RBP functions in cell proliferation and mitotic cell division. This hypothesis is further demonstrated by the reduced rate of cell proliferation that we found in embryos and in primary cultures of embryonic fibroblasts derived from null mice compared to their littermates (data not shown). However, the normal development of B and T cells in TB-RBP-null mice was unexpected, suggesting that an alternative system exists for the critical lymphocyte processes of immunoglobulin or TcR rearrangements in mice as well as the proliferative bursts known to occur in early B- and T-cell development (20, 30, 48, 53). Thus, while TB-RBP plays a key role in proliferation in many tissues, in developing lymphoid progenitors, alternative mediators can regulate DNA recombination and cell division in the absence of TB-RBP. Similarly, there were no differences in mitotic proliferation in the spermatogenic cycle in testes from wild-type or TB-RBP-null mice (data not shown).

The abundance of TB-RBP in testis and brain led us to predict major disruptions in both of these organs in null animal. Although the null male mice bred and produced normally sized litters, spermatogenesis was severely affected, and a progressive reduction in sperm numbers was observed. The high level of cell death in meiotic prophase and especially at metaphase 1 is consistent with a microtubule function for TB-RBP. Despite the abnormal spermatogenesis and vacuolization seen in null males, fertility was maintained, suggesting that male germ cells contain redundant pathways to regulate the transport and temporal expression of posttranscriptionally regulated mRNAs. A number of RNA-binding proteins, e.g., MSY2, MSY4, and Prbp, are known to bind to the 3′ untranslated regions of translationally delayed testicular mRNAs, such as protamine mRNAs, and affect their translation (reviewed in references 9 and 21). These findings suggest that multiple systems exist to regulate posttranscriptional germ cell functions such as mRNA transport and translation.

TB-RBP exhibits many functional similarities with the fragile X syndrome protein (FMRP), such as involvement in nuclear export and localization of mRNAs. TB-RBP is associated with translationally delayed messages during nuclear export and is present in multiprotein nonpolysomal RNP complexes during the transport or translational delay of specific mRNAs (41). Inhibition of FMRP leads to mild cognitive deficiencies in mice, with translational misregulation of mRNAs associated with FMRP being postulated to be the cause for the FMRP phenotype. Recently, by use of microarray analysis, it was shown that the polysome profile of mRNAs is altered in FMRP-null mice (10). In the brains of TB-RBP-null mice, both FMRP and FXR1 mRNAs were down-regulated, 3.4- and 2.2-fold, respectively. Moreover, RNA targets of FMRP, such as the tetratrichopeptide repeat protein (Table 2, additional genes) and the GAP-associated protein p190-B (Table 2, G protein signaling) (10), were also down-regulated in the brains of TB-RBP-null mice. Although there is not likely a direct association of FMRP-containing mRNPs with TB-RBP-associated mRNAs, both proteins may have overlapping functions in mRNA localization in the brain.

TB-RBP is an RNA-binding protein known to preferentially bind to a consensus sequence present in a number of testis and brain mRNAs. In the testis, TB-RBP binds to a number of mRNAs, including those for protamines 1 and 2, AKAP4, and glyceraldehyde 3-phosphate dehydrogenase S (32, 41, 60). In the brain, TB-RBP-binding elements in the 3′ untranslated regions of myelin basic protein and calcium- or calmodulin-dependent protein kinase IIα have been identified (59). Although many mRNAs were down-regulated in the brains of TB-RBP-null animals, no obvious Y and H sequence-binding

sites of TB-RBP were detected in the down-regulated brain mRNAs. By use of RT-PCR to assay for immunoprecipitated mRNAs, myelin basic protein mRNA, a known target of TB-RBP, was selectively precipitated (59). However, several of the markedly down-regulated mRNAs (GABA-A receptor α1, glutamate receptor α3, synaptobrevin, and matrin 3) were not detectable in the TB-RBP immunoprecipitates (data not shown). These results suggest that the down-regulation of many of the brain mRNAs in TB-RBP-null mice is not due to a direct interaction or stabilization of these mRNAs by TB-RBP. It is also possible that TB-RBP functions in nuclear pre-mRNA processing and/or export. For example, in previous studies, a functional leucine-rich nuclear export signal and a TB-RBP association with specific mRNAs during the nuclear export of TB-RBP in male germ cells were found (12, 41). Several of the genes with altered expression in the brains of TB-RBP-null mice may indicate that there are compensatory mechanisms to counteract the functional loss of TB-RBP or TRAX. The down-regulation of MAP-2, for instance, may restore the microtubule motility that may be negatively affected due to the absence of TB-RBP (36). The down-regulation in null mice of the NIMA (never in mitosis gene A) kinase (Table 2), which phosphorylates MAP-2, may indicate multiple levels of gene regulation.

The suppression of TB-RBP by antisense oligonucleotides disrupts and mislocalizes specific mRNA sorting in cultured rat hippocampal cells (46). Although we did not detect any major morphological changes in the brains of TB-RBP-null mice by light microscopy, we did detect major alterations in gene expression. Most of these changes represented the down-regulation of specific mRNAs, while a few mRNAs were up-regulated in the brains of null mice. The changes in brain mRNA levels induced by the disruption of TB-RBP likely contribute to the changes in behavior that we detected. Performance over multiple trials on the accelerating Rota-Rod is used to measure cerebellum-dependent motor coordination and motor learning (25). Mutant mice with known defects in cerebellar neuroanatomy, such as *staggerer*, *hot-foot*, and *lurcher* mice, show severely impaired performance that does not improve across trials (34). TB-RBP-null mice exhibited a more subtle phenotype; their performance improved over time, but their mean latency to falling was consistently shorter than that of their wild-type littermates. TB-RBP knockout mice had normal cerebellar anatomy (data not shown), but changes in the levels of expression of various mRNAs, particularly those encoding GABA-A receptor subunits, may produce functional differences in cerebellar circuitry (Table 2). Cerebellar granule cells receive inhibitory feedback from Golgi neurons at synapses containing α1β2/3γ2 and α6β2/3γ2 GABA-A receptor subunit combinations (43). The α6 subunit is exclusively expressed in cerebellar and cochlear nucleus granule cells (27). Both α1 and α6 subunit mRNA levels were significantly decreased in TB-RBP-null mice. Surprisingly, knockout mice lacking either the α1 or the α6 subunit were not significantly impaired in the Rota-Rod task (29, 49). The significant deficit in the TB-RBP-null mice may reflect the combined effects of decreased α1 and α6 subunit expression, but both α1 and α6 subunit knockout mice also have some decreased expression of the complementary cerebellar GABA-A α receptor (49, 51). Differences in the Rota-Rod apparatus and testing procedures make it difficult to compare between experiments; more extensive training at lower Rota-Rod speeds could explain the lack of an observed deficit in α1 subunit- and α6 subunit-deficient mice.

Importantly, Rota-Rod performance is also sensitive to other factors, such as muscle strength and fatigability. Thus, the Rota-Rod deficits in TB-RBP-null mice could also reflect peripheral functions of TB-RBP. Although the mice were not grossly impaired, the observed reduction in lean body mass (see below) could have affected their performance on a demanding motor task. Hence, the Rota-Rod deficits could also be due to metabolic impairments. TB-RBP knockout mice displayed normal swim speeds in the Morris Water maze and thus were not grossly impaired in a less demanding motor task over a shorter time period (1 min) (data not shown). Moreover, the numerous changes in brain mRNA levels suggest that multiple systems and additional brain regions may be affected in these mice, and analysis of other behavioral phenotypes is ongoing.

The absence of TB-RBP appears to result in a mild decrease in skeletal muscle, as lean body mass, an indicator of total skeletal muscle mass, is reduced in null mice. In addition, a loose skin phenotype related to abnormalities in the panniculus carnosus, a subcutaneous striated muscle layer, was detected (data not shown). In addition, we observed a disproportionate accumulation of visceral fat in TB-RBP-null mice. This visceral fat may exacerbate the reduced fertility seen in null females. There are a number of causes of visceral obesity; however, it is generally thought to be a result of a neuroendocrine disorder associated with hypothalamic-pituitary-adrenal axis dysregulation (7) or elevated muscle sympathetic nerve activity (2). Common endocrine disorders associated with excess visceral fat are decreased growth hormone secretion (8) and exposure to excessive levels of glucocorticoids (38, 54). The observation that bone density was normal in TB-RBP-null mice argues against an excess of systemic glucocorticoids, as this defect causes marked osteopenia. However, it is possible that the absence of TB-RBP induces an adipose tissue-specific abnormality in glucocorticoid action or metabolism, resulting in elevated levels of corticosterone (37), which in turn would induce an accumulation of visceral fat. Future studies will be necessary to determine whether this or other mechanisms are responsible.

Although TB-RBP is expressed in both germ cells and somatic cells in the female reproductive tract, the process of fertilization appears not to be impaired in null females. Histological analyses of stained sections of ovaries and uteri of wild-type and null mice did not reveal obvious defects. The reduced fertility was variable, with one null female repeatedly producing normally sized litters, while several null females failed to produce any offspring after more than a year of mating with different experienced wild-type and heterozygous males. The cause of the decreased litter sizes in null females is under investigation.

We do not know whether the phenotypes seen when TB-RBP is inhibited result from the absence of TB-RBP, the absence of TRAX, or their coordinate loss. The reduction of TB-RBP in heterozygotes and its absence in homozygotes leads to an equivalent reduction of TRAX. This reduction in TRAX occurs at a posttranscriptional level, since TRAX

mRNA levels are not substantially decreased in the heterozygote and TB-RBP-null animals (Fig. 3). Attempts to overexpress TRAX in male germ cells by transgenesis resulted in a coordinate decrease in the level of endogenous TRAX, suggesting a stabilizing role for TB-RBP (unpublished data). Although Translin shows 98% identity between mice and humans, TRAX is less conserved between these species, with 90% identity (4). However, both proteins show a high degree of cross-species conservation and are concomitantly expressed in mammals, insects, and yeasts. We believe that the loss of TRAX in the absence of TB-RBP is due to their need for an interaction, as TRAX is normally stabilized in a complex by TB-RBP. Preliminary transfection studies with embryonic fibroblasts from null mice have indicated that TRAX reappears with the reintroduction of TB-RBP (S. Yang and N. B. Hecht, unpublished data). Although TB-RBP and TRAX form heterooligomers in vitro (12) and Translin-TRAX complexes that bind GSI strand-specific DNA and RNA have been detected in the brain (17), it is likely that TB-RBP and TRAX have additional protein partners and individual functions. TRAX contains a putative bipartite nuclear targeting sequence, suggesting that TRAX could facilitate the movement of protein into nuclei. In fact, following DNA damage, direct TRAX interactions with CID have been demonstrated without TB-RBP involvement (14, 15). Thus, it is difficult to know whether the phenotypes that we find in the TB-RBP-null mice result from deficiencies in TB-RBP, TRAX, or both. The correlation between increased cellular proliferation and increased TB-RBP in cultured cells (22) suggests that the growth retardation seen in TB-RBP-null mice is caused at least by a TB-RBP deficiency. Ongoing studies with transgenic mice and cell lines derived from TB-RBP-null mice and their littermates promise to dissect the shared and distinct functions of TB-RBP and TRAX.

ACKNOWLEDGMENTS

This work was supported by NIH grant HD 28832 (to N.B.H.).

We thank G. Radice (University of Pennsylvania) and M. A. Handel (University of Tennessee) for numerous valuable discussions and suggestions, J. Golden (Children's Hospital of Pennsylvania) for examination of tissue sections, M. Meistrich (M. D. Anderson Hospital) for analysis of the cycle of the seminiferous epithelium, members of the laboratory of G. Gerton for introducing us to sperm quantitation methods, Y. Fang for help with behavioral analyses, and D. Adamoli for excellent secretarial assistance.

REFERENCES

1. **Allman, D., R. C. Lindsley, W. De Muth, K. Rudd, S. A. Shinton, and R. R. Hardy.** 2001. Resolution of three nonproliferative immature splenic B cell subsets reveals multiple selection points during peripheral B cell maturation. J. Immunol. **167:**6834–6840.
2. **Alvarez, G. E., S. D. Beske, T. P. Ballard, and K. P. Davy.** 2002. Sympathetic neural activation in visceral obesity. Circulation **106:**2533–2536.
3. **Aoki, K., J. Inazawa, T. Takahashi, K. Nakahara, and M. Kasai.** 1997. Genomic structure and chromosomal localization of the gene encoding translin, a recombination hotspot binding protein. Genomics **43:**237–241.
4. **Aoki, K., R. Ishida, and M. Kasai.** 1997. Isolation and characterization of a cDNA encoding a Translin-like protein TRAX. FEBS Lett. **401:**109–112.
5. **Aoki, K., K. Suzuki, R. Ishida, and M. Kasai.** 1999. The DNA binding activity of Translin is mediated by a basic region in the ring-shaped structure conserved in evolution. FEBS Lett. **443:**363–366.
6. **Aoki, K., K. Suzuki, T. Sugano, T. Tasaka, K. Nakahara, O. Kuge, A. Omori, and M. Kasai.** 1995. A novel gene, Translin, encodes a recombination hotspot binding protein associated with chromosomal translocations. Nat. Genet. **10:**167–174.
7. **Bjorntorp, P., and R. Rosmond.** 2000. Neuroendocrine abnormalities in visceral obesity. Int. J. Obes. Relat. Metab. Disord. **24**(Suppl. 2)**:**S80–S85.
8. **Bosello, O., and M. Zamboni.** 2000. Visceral obesity and metabolic syndrome. Obes. Rev. **1:**47–56.
9. **Braun, R. E.** 2000. Temporal control of protein synthesis during spermatogenesis. Int. J. Androl. **23:**92–94.
10. **Brown, V., P. Jin, S. Ceman, J. C. Darnell, W. T. O'Donnell, S. A. Tenenbaum, X. Jin, Y. I. Feng, K. D. Wilkinson, J. D. Keene, R. B. Darnell, and S. T. Warren.** 2001. Microrray identification of FMRP-associated brain mRNAs and altered mRNA translational profiles in fragile X syndrome. Cell **107:**477–487.
11. **Caudy, A. A., M. Myers, G. J. Hannon, and S. M. Hammond.** 2002. Fragile X-related protein and VIG associate with the RNA interference machinery. Genes Dev. **16:**2492–2496.
12. **Chennathukuzhi, V. M., Y. Kurihara, J. D. Bray, and N. B. Hecht.** 2001. Trax (Translin associated factor X), a primarily cytoplasmic protein, inhibits the binding of TB-RBP (Translin) to RNA. J. Biol. Chem. **276:**13256–13263.
13. **Chennathukuzhi, V. M., Y. Kurihara, J. D. Bray, J. Yang, and N. B. Hecht.** 2001. Altering the GTP binding site of the DNA/RNA-binding protein, Translin/TB-RBP, decreases RNA binding and may create a dominant negative phenotype. Nucleic Acids Res. **29:**4433–4440.
14. **Erdemir, T., B. Bilican, T. Cagatay, C. R. Goding, and U. Yavuzer.** 2002. *Saccharomyces cerevisiae* C1D is implicated in both non-homologous DNA end joining and homologous recombination. Mol. Microbiol. **46:**947–957.
15. **Erdemir, T., B. Bilican, D. Oncel, C. R. Goding, and U. Yavuzer.** 2002. DNA damage-dependent interaction of the nuclear matrix protein C1D with Translin associated factor X (TRAX). J. Cell Sci. **115:**207–216.
16. **Finkenstadt, P. M., M. Jeon, and J. M. Baraban.** 2001. Masking of the Translin/Trax complex by endogenous RNA. FEBS Lett. **498:**6–10.
17. **Finkenstadt, P. M., W. S. Kang, M. Jeon, E. Taira, W. Tang, and J. M. Baraban.** 2000. Somatodendritic localization of Translin, a component of the Translin/Trax RNA binding complex. J. Neurochem. **75:**1754–1762.
18. **Han, J. R., W. Gu, and N. B. Hecht.** 1995. Testis-brain RNA-binding protein, a testicular translational regulatory RNA-binding protein, is present in the brain and binds to the 3′ untranslated regions of transported brain mRNAs. Biol. Reprod. **53:**707–717.
19. **Han, J. R., K. C. Yiu, and N. B. Hecht.** 1995. Testis/brain RNA-binding protein attaches translationally repressed and transported mRNAs to microtubules. Proc. Natl. Acad. Sci. USA **92:**9550–9554.
20. **Hardy, R. R., Y. S. Li, D. Allman, M. Asano, M. Gui, and K. Hayakawa.** 2000. B-cell commitment, development and selection. Immunol. Rev. **175:**23–32.
21. **Hecht, N. B.** 1998. Molecular basis of male germ cell differentiation. Bioessays **20:**555–561.
22. **Ishida, R., H. Okado, H. Sato, C. Shinonoiri, K. Aoki, and M. Kasai.** 2002. A role for the octameric ring protein, Translin, in mitotic cell division. FEBS Lett. **525:**105–110.
23. **Ishizuka, A., M. C. Siomi, and H. Siomi.** 2002. A *Drosophila* fragile X protein interacts with components of RNAi and ribosomal proteins. Genes Dev. **16:**2497–2508.
24. **Izon, D., K. Rudd, W. DeMuth, C. Clendenin, R. C. Lindsley, and D. Allman.** 2001. A common pathway for dendritic cell and earl B cell development. J. Immunol. **167:**1387–1392.
25. **Jones, B. J., and D. J. Roberts.** 1968. A rotarod suitable for quantitation measurements of motor incoordination in naïve mice. Naunyn-Schmiedeberg's Arch. Pharmacol. **259:**211.
26. **Kasai, M., T. Matsuzaki, K. Katayanagi, A. Omori, R. T. Maziarz, J. L. Strominger, K. Aoki, and K. Suzuki.** 1997. The translin ring specifically recognized DNA ends at recombination hot spots in the human genome. J. Biol. Chem. **272:**11402–11407.
27. **Kato, K.** 1990. Novel $GABA_A$ receptor α subunit is expressed only in cerebellar granule cells. J. Mol. Biol. **214:**619–624.
28. **Kobayashi, S., A. Takashima, and K. Anzai.** 1998. The dendritic translocation of translin protein in the form of BC1 RNA protein particles in developing rat hippocampal neurons in primary culture. Biochem. Biophys. Res. Commun. **253:**448–453.
29. **Korpi, E. R., P. Koikkalainen, O. Y. Vekovischeva, R. Makela, R. Kleinz, M. Uusi-Oukari, and W. Wisden.** 1998. Cerebellar granule-cell-specific $GABA_A$ receptors attenuate benzodiazepine-induced ataxia: evidence from α6-subunit deficient mice. Eur. J. Neurosci. **11:**233–240.
30. **Kruisbeek, A. M.** 1993. Development of alpha beta T cells. Curr. Opin. Immunol. **5:**227–234.
31. **Kwon, K. Y., and N. B. Hecht.** 1991. Cytoplasmic protein binding to highly conserved sequences in the 3′ untranslated region of mouse protamine 2 mRNA, a translationally regulated gene of male germ cells. Proc. Natl. Acad. Sci. USA **88:**3584–3588.
32. **Kwon, K. Y., and N. B. Hecht.** 1993. Binding of a phosphoprotein to the 3′ untranslated region of the mouse protamine 2 mRNA temporally represses its translation. Mol. Cell. Biol. **13:**6547–6557.
33. **Laird, P. W., A. Zijderveld, K. Linders, M. A. Rudnicki, R. Jaenisch, and A. Berns.** 1991. Simplified mammalian DNA isolation procedure. Nucleic Acids Res. **19:**4293–4295.
34. **Lalonde, R., M. Filali, A. N. Bensoula, and F. Lestienne.** 1996. Sensorimotor learning in three cerebellar mutant mice. Neurobiol. Learn. Mem. **65:**113–120.

35. **Lee, S. P., E. Fuior, M. S. Lewis, and M. K. Han.** 2001. Analytical ultracentrifugation studies of Translin: analysis of protein-DNA interactions using a single-stranded fluorogenic oligonucleotide. Biochemistry **40:**14081–14088.
36. **Lopez, L. A., and M. P. Sheetz.**. 1995. Amicrotubule-associated protein (MAP2) kinase restores microtubule motility in embryonic brain. J. Biol. Chem. **270:**12511–12517.
37. **Masusaki, H., J. Paterson, H. Shinyama, N. M. Morton, J. J. Mullins, J. R. Seckl, and J. S. Flier.** 2001. A transgenic model of visceral obesity and the metabolic syndrome. Science **294:**2166–2170.
38. **Mayo-Smith, W., C. W. Hayes, B. M. K. Biller, A. Klibanski, H. Rosenthal, and D. I. Rosenthal.** 1989. Body fat distribution measured with CT: correlation in healthy subjects, patients with anorexia nervosa, and patients with Cushing's syndrome. Radiology **170:**515–518.
39. **Mombaerts, P., J. Iacomini, R. S. Johnson, K. Herrup, S. Tonegawa, and V. Papaioannou.** 1992. RAG-1-deficient mice have no mature B and T lymphocytes. Cell **68:**869–877.
40. **Morales, C. R., S. Lefrancois, V. Chennathukuzhi, M. El-Alfy, X.-Q. Wu, J. Yang, G. L. Gerton, and N. B. Hecht.** 2002. A TB-RBP and Ter ATPase complex accompanies specific mRNAs from nuclei through the nuclear pores and into intercellular bridges in mouse male germ cells. Dev. Biol. **246:**480–494.
41. **Morales, C. R., X.-Q. Wu, and N. B. Hecht.** 1998. The DNA/RNA-binding protein, TB-RBP, moves from the nucleus to the cytoplasm and through intercellular bridges in male germ cells. Dev. Biol. **201:**113–123.
42. **Narisawa, S., N. Frohlander, and J. L. Millan.** 1997. Inactivation of two mouse alkaline phosphatase genes and establishment of a model of infantile hypophosphatasia. Dev. Dyn. **208:**432–446.
43. **Nusser, Z., W. Sieghart, and P. Somogyi.** 1998. Segregation of different $GABA_A$ receptors to synaptic and extrasynaptic membranes of cerebellar granule cells. J. Neurosci. **18:**1693–1703.
44. **Pascal, J. M., V. M. Chennathukuzhi, N. B. Hecht, and J. D. Robertus.** 2001. Mouse testis-brain RNA-binding protein (TB-RBP): expression, purification, and crystal X-ray diffraction. Acta Crystallogr. Sect. D **57:**1692–1694.
45. **Sengupta, K., and B. J. Rao.** 2002. Translin binding to DNA: recruitment through DNA ends and consequent conformational transitions. Biochemistry **41:**15315–15326.
46. **Severt, W. L., T. Biber, X.-Q. Wu, N. B. Hecht, R. J. Delorenzo, and E. R. Jakoi.** 1999. The suppression of testis-brain RNA binding protein and kinesin heavy chain disrupts mRNA sorting in dendrites. J. Cell Sci. **112:**3691–3702.
47. **Shinkai, Y., G. Rathbun, K. P. Lam, E. M. Oltz, V. Stewart, M. Mendelsohn, J. Charion, M. Dotta, F. Young, and A. M. Stall.** 1992. RAG-2-deficient mice lack mature lymphocytes owing to inability to initiate V(D)J rearrangement. Cell **68:**855–867.
48. **Spanopoulou, E., C. A. Roman, L. M. Corcoran, M. S. Schlissel, D. P. Silver, D. Nemazee, M. C. Nussenzweig, S. A. Shinton, R. R. Hardy, and D. Baltimore.** 1994. Functional immunoglobulin transgenes guide ordered B-cell differentiation in Rag-1-deficient mice. Genes Dev. **8:**1030–1042.
49. **Sur, C., K. A. Wafford, D. S. Reynolds, K. L. Hadingham, F. Bromidge, A. Macaulay, N. Collinson, G. O'Meara, O. Howell, R. Newman, J. Myers, J. R. Atack, G. R. Dawson, R. M. McKernan, P. J. Whiting, and T. W. Rosahl.** 2001. Loss of the major GABAA receptor subtype in the brain is not lethal in mice. J. Neurosci. **21:**3409–3418.
50. **Travis, A. J., J. A. Foster, N. A. Rosenbaum, P. E. Visconti, G. L. Gerton, G. S. Kopf, and S. B. Moss.** 1998. Targeting of a germ cell-specific type 1 hexokinase lacking a porin-binding domain to the mitochondria as well as to the head and fibrous sheath of murine spermatozoa. Mol. Biol. Cell **9:**263–276.
51. **Uusi-Oukari, M., J. Heikkila, S. T. Sinkkonen, R. Makela, B. Hauer, G. E. Homanics, W. Sieghart, W. Wisden, and E. R. Korpi.** 2000. Long-range interactions in neuronal gene expression: evidence from gene targeting in the GABAA receptor β2-α6-α1-γ2 subunit gene cluster. Mol. Cell. Neurosci. **16:**34–41.
52. **VanLoock, M. S., X. Yu, M. Kasai, and E. H. Elgeman.** 2001. Electron microscopic studies of the Translin octameric ring. J. Struct. Biol. **135:**58–66.
53. **von Boehmer, H., and H. J. Fehling.** 1997. Structure and function of the pre-T cell receptor. Annu. Rev. Immunol. **15:**433–452.
54. **Wajchenberg, B. L.** 2000. Subcutaneous and visceral adipose tissue: their relation to the metabolic syndrome. Endocrinol. Rev. **21:**697.
55. **Wu, W.-Q., W. Gu, X.-H. Meng, and N. B. Hecht.** 1997. The RNA-binding protein, TB-RBP, is the mouse homologue of translin, a recombination protein associated with chromosomal translocations. Proc. Natl. Acad. Sci. USA **94:**5640–5645.
56. **Wu, W.-Q., L. Xu, and N. B. Hecht.** 1998. Dimerization of the testis brain RNA-binding protein (Translin) is mediated through its C-terminus and is required for DNA and RNA binding. Nucleic Acids Res. **26:**1675–1680.
57. **Wu, X.-Q., S. Lefrancois, C. R. Morales, and N. B. Hecht.** 1999. Protein-protein interactions between the testis brain RNA-binding protein and the transitional endoplasmic reticulum ATPase, a cytoskeletal γ actin and Trax in male germ cells and the brain. Biochemistry **38:**11261–11270.
58. **Wu, X.-Q., P. Petrusz, and N. B. Hecht.** 1999. Testis brain RNA-binding protein (Translin) is primarily expressed in neurons of the mouse brain. Brain Res. **819:**174–178.
59. **Wu, X. Q., and N. B. Hecht.** 2000. Mouse testis brain RNA-binding protein (TB-RBP) colocalizes with microtubules and immunoprecipitates with mRNAs encoding myelin basic protein, α calmodulin kinase II and protamines 1 and 2. Biol. Reprod. **62:**720–725.
60. **Yang, J., V. Chennathukuzhi, K. Miki, D. A. O'Brien, and N. B. Hecht.** 2003. Mouse TB-RBP/Translin selectively binds to the mRNA of the fibrous sheath protein, glyceraldehyde 3-phosphate dehydrogenase-S, and suppresses its translation *in vitro*. Biol. Reprod. **68:**853–859.
61. **Zambrowicz, B. P., G. A. Friedrich, E. C. Buxton, S. L. Lilleberg, C. Person, and A. T. Sands.** 1998. Disruption and sequence identification of 2, 000 genes in mouse embryonic stem cells. Nature **392:**608–611.
62. **Zambrowicz, B. P., A. Imamoto, S. Fiering, L. A. Herzenberg, W. G. Kerr, and P. Soriano.** 1997. Disruption of overlapping transcripts in the ROSA βgeo 26 gene trap strain leads to widespread expression of β-galactosidase in mouse embryos and hematopoietic cells. Proc. Natl. Acad. Sci. USA **94:**3789–3794.